ADVANCED MATERIALS

www.advmat.de

Revisiting the Buckling Metrology Method to Determine the Young's Modulus of 2D Materials

*Nestor Iguiñiz, Riccardo Frisenda, Rudolf Bratschitsch, and Andres Castellanos-Gomez**

Measuring the mechanical properties of 2D materials is a formidable task. While regular electrical and optical probing techniques are suitable even for atomically thin materials, conventional mechanical tests cannot be directly applied. Therefore, new mechanical testing techniques need to be developed. Up to now, the most widespread approaches require micro-fabrication to create freely suspended membranes, rendering their implementation complex and costly. Here, a simple yet powerful technique is revisited to measure the mechanical properties of thin films. The buckling metrology method, that does not require the fabrication of freely suspended structures, is used to determine the Young's modulus of several transition metal dichalcogenides (MoS_2, $MoSe_2$, WS_2, and WSe_2) with thicknesses ranging from 2 to 10 layers. The obtained values for the Young's modulus and their uncertainty are critically compared with previously published results, finding that this simple technique provides results which are in good agreement with those reported using other highly sophisticated testing methods. By comparing the cost, complexity, and time required for the different methods reported in the literature, the buckling metrology method presents certain advantages that make it an interesting mechanical test tool for 2D materials.

2D materials are promising candidates for future flexible electronics applications due to their combination of remarkable mechanical and electrical properties.[1] In fact, from the mechanics point of view, 2D materials are similar to polymers, as they are very elastic and resilient to large deformations,[2,3] while keeping electronic performance comparable to that of crystalline 3D materials.[4,5]

While the electrical and optical properties of 2D materials can be explored with conventional experimental tools developed to test 3D materials and thin film devices, probing the mechanical properties of 2D materials is more challenging, as neither bending nor tensile test macroscopic setups can be employed. Nanoindentation,[2,6–8] the analysis of the dynamics of nanomechanical resonators,[9] and the microscopic adaptation of tensile tests setups[10] or Brillouin scattering[11] have been developed to characterize the fundamental mechanical properties of 2D materials such as their Young's modulus.[12,13] Although powerful, these techniques require dedicated setups and rather complex data acquisition and/or analysis. Alternative to these methods, Stafford et al.[14] introduced the buckling metrology method, a simple and elegant way to measure the Young's modulus of thin polymeric films by studying the buckling instability, which arises when the film is deposited onto a compliant substrate, and it is subjected to uniaxial compression.[15] Under these conditions, the trade-off between the adhesion forces between film and substrate and the bending rigidity of the film leads to a rippling of the thin film with a characteristic wavelength that only depends on the elastic properties of the film and the substrate. This elegant method to characterize the mechanical properties of thin films has been extensively used to study coatings[14] and organic semiconducting materials.[16] However, it has been scarcely employed to study 2D materials,[17–20] and it seems that is has been mostly overlooked by the 2D materials community.

Here, we apply the buckling-based metrology method to determine the Young's modulus of transition metal dichalcogenide (TMDC) flakes with thickness ranging from 2 layers up to 10 layers. We use optical microscopy to determine both the number of layers and the rippling wavelength, which is therefore very fast and simple to implement. We critically compare the results obtained with this method and demonstrate that despite its simplicity it provides results in good agreement with other techniques to study the mechanical properties of 2D materials. We believe that the buckling-based metrology method provides a fast route to determine the Young's modulus of 2D materials, being an excellent alternative to other existing nanomechanical test methods that are more technically demanding.

The samples are fabricated by mechanical exfoliation of bulk layered TMDC crystals with adhesive tape (see Experimental Section for details). The exfoliated material is then transferred onto a compliant elastomeric substrate (Gel-Film, a commercially available polydimethylsiloxane, PDMS, film manufactured by Gel-Pak) which is subjected to a uniaxial stress of ≈20%. Right after the transfer, the stress on the elastomeric

N. Iguiñiz, Dr. R. Frisenda, Dr. A. Castellanos-Gomez
Materials Science Factory, Instituto de Ciencia de Materiales de Madrid (ICMM)
Consejo Superior de Investigaciones Científicas (CSIC)
Sor Juana Inés de la Cruz, 3
28049 Madrid, Spain
E-mail: andres.castellanos@csic.es

Prof. R. Bratschitsch
Institute of Physics and Center for Nanotechnology
University of Münster
48149 Münster, Germany

The ORCID identification number(s) for the author(s) of this article can be found under https://doi.org/10.1002/adma.201807150.

DOI: 10.1002/adma.201807150

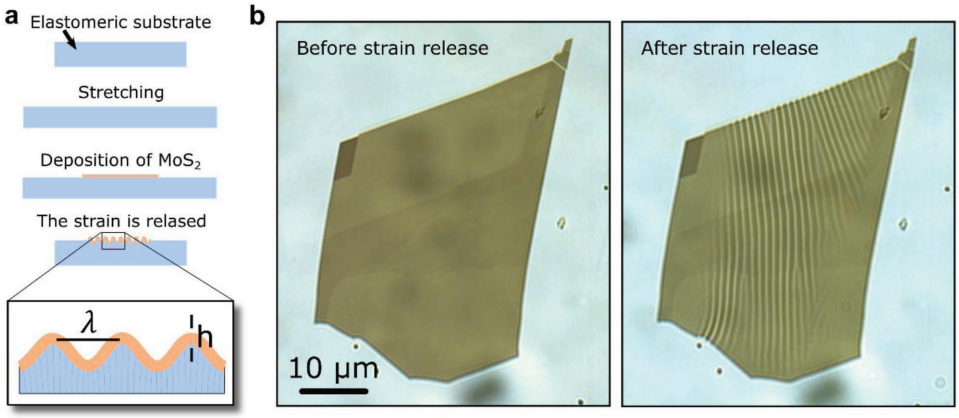

Figure 1. a) Sketch of the process employed to fabricate the samples used in the buckling metrology method. The flakes are transferred onto a stressed elastomeric substrate, when the stress on the substrate is released the flakes are subjected to uniaxial compressive strain that produces the buckling of the flakes. b) Transmission mode optical microscopy images of a MoS_2 multilayer flake (the thinner region is 7L thick) before and after releasing the stress on the elastomeric substrate.

substrate is released, yielding to compressive uniaxial strain of the transferred flakes (**Figure 1**a shows a schematic diagram of the sample fabrication process). Note that due to the large Young's modulus mismatch between the elastomeric substrate and the 2D materials only a small fraction of the substrate pre-stress will be transferred to the flakes after releasing the stress. Figure 1b displays transmission mode optical microscopy images of a multilayered MoS_2 flake after being transferred onto the pre-stressed elastomeric substrate and right after releasing the stress on the substrate.

The rippled pattern arises from the buckling instability resulting from the balance between the energy required to bend the stiff 2D material, the energy to elastically deform the soft underlying Gel-Film and the adhesion energy between them. Interestingly, the wavelength of these ripples is independent on the initial pre-stress of the elastomeric substrate and it only depends on the materials properties of both flake and substrate[14,21,22]

$$\lambda = 2\pi h \left[\frac{\left(1-\nu_s^2\right)E_f}{3\left(1-\nu_f^2\right)E_s} \right]^{1/3} \quad (1)$$

where h is the flake thickness, ν_s and ν_f are the Poisson's ratio of substrate and flake and E_s and E_f are the Young's modulus of the substrate and flake, respectively. This equation is valid under certain assumptions: a) the flake should follow a sinusoidal rippling, b) $E_f/E_s >> 1$, c) the substrate should be much thicker than the flake, d) the amplitude of the ripples should be much smaller than their wavelength (thus the shear forces are neglected), e) the adhesion between the flake and substrate is strong enough to prevent slippage, and f) all the deformations are assumed to be elastic.

According to Equation (1) spatial wavelength of the ripples monotonically depends on the thickness of the flakes, as the other parameters are fixed and they only depend on the intrinsic mechanical properties of the substrate and flake materials. **Figure 2** shows a comparison between the rippled pattern observed in 3, 7, and 10L MoS_2 flakes whose thickness is determined via quantitative analysis of their transmittance[23] (see Supporting Information). The optical microscopy-based thickness determination method provides accurate thickness values for flakes in the 1 to 10 layers range. For thicker flakes the absorption starts to saturate and thus the thickness uncertainty rapidly increases.

Using Equation (1), the Young's modulus of the deposited 2D materials can be determined by measuring the thickness-dependent ripple period provided that ν_s, ν_f, and E_s are known values. The Poisson's ratio of the Gel-Film (PDMS) substrate $\nu_s = 0.5$[24] and flake $\nu_f = 0.27$[25,26] are found in the literature, with low spread in their values. Moreover, the Young's modulus is rather insensitive to small variations of the Poisson's ratio (see Figure S11, Supporting Information). Because the PDMS Young's modulus values given in the literature show a large scattering (from 300 to 1000 kPa, strongly dependent on the curing process),[27,28] we have experimentally determined the Young's modulus of our Gel-Film substrate E_s = 492 ± 11 kPa (see Experimental Section and Supporting Information for more details about the Gel-Film Young's modulus determination). The Young's modulus of MoS_2 can be determined from the slope of the linear relationship between the ripple period (λ) and the flake thickness (h) as follows:

$$E_f = \frac{3\left(1-\nu_f^2\right)E_s}{8\pi^3\left(1-\nu_s^2\right)}\left[\frac{\lambda}{h}\right]^3 \quad (2)$$

Figure 3a displays the measured ripple period and the flake thickness, determined from the analysis of the transmission mode optical images, of flakes 3 to 10 layers thick. Note that flakes thinner than 3 layers present ripples with a period <0.6 μm and a small amplitude (<6 nm) that cannot be resolved with optical microscopy (see the Supporting Information) and flakes thicker than ≈10 layers typically yield very large flake-to-flake variation of their mechanical properties which has been attributed to the presence of stacking faults.[12,29,30] In order to resolve the ripples in flakes thinner than 3 layers one can alternatively use AFM (see some experimental data points

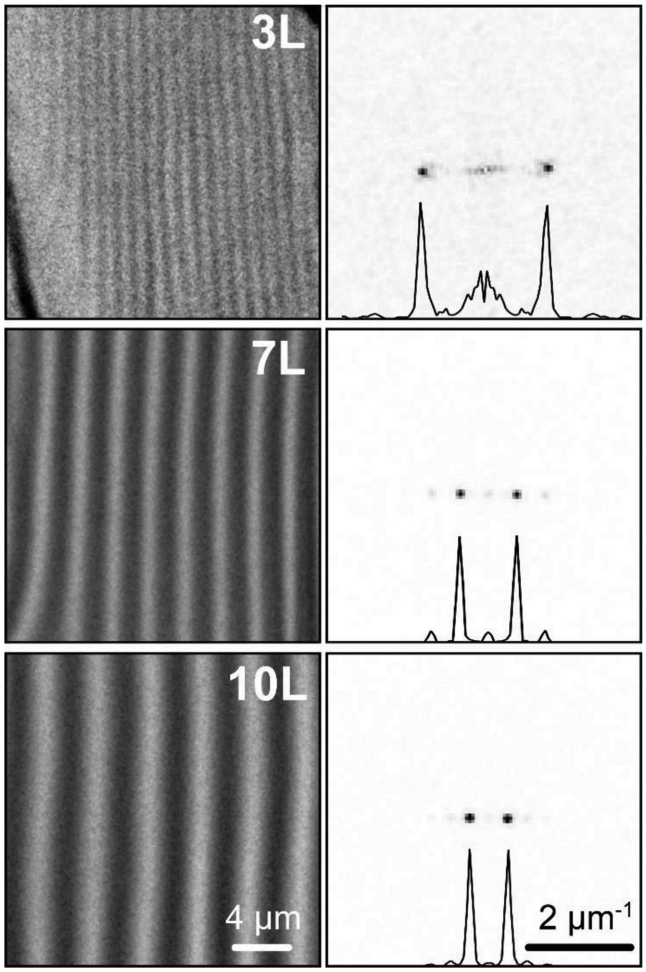

Figure 2. Grayscale white-light transmission mode optical microscopy images of the rippled pattern observed in 3, 7, and 10L MoS_2 flakes and their corresponding FFTs. Line cuts along the FFT maxima are included in the FFT panels.

acquired by measuring the ripple wavelength through AFM in Figure 3a and its associated discussion in the Supporting Information). The experimental data follows a clear linear trend, in agreement with Equation (1) and from its slope we determine E_f following Equation (2): $E_f = 246 \pm 35$ GPa (see Supporting Information for a discussion about the uncertainty determination). We observed a relatively large flake-to-flake variation of the ripple period (i.e., flakes with same thickness yield sizeably different ripple periods), which we attribute to the presence of small defects such as folds or wrinkles in some of the flakes. Therefore, measurements of several flakes with different thicknesses are needed to obtain a well-defined Young's modulus value with a low uncertainty. We found that measurements over at least 6–8 flakes (with ≥4 different thicknesses) are needed to determine the Young's modulus with an uncertainty comparable to that obtained with other mechanical testing techniques like nanoindentation (see Figure S9 and Table S3, Supporting Information).

This Young's modulus value is in good agreement with the values reported in the literature, determined through different experimental techniques. Figure 3b shows a comparison between the different values of the Young's modulus for few-layer MoS_2

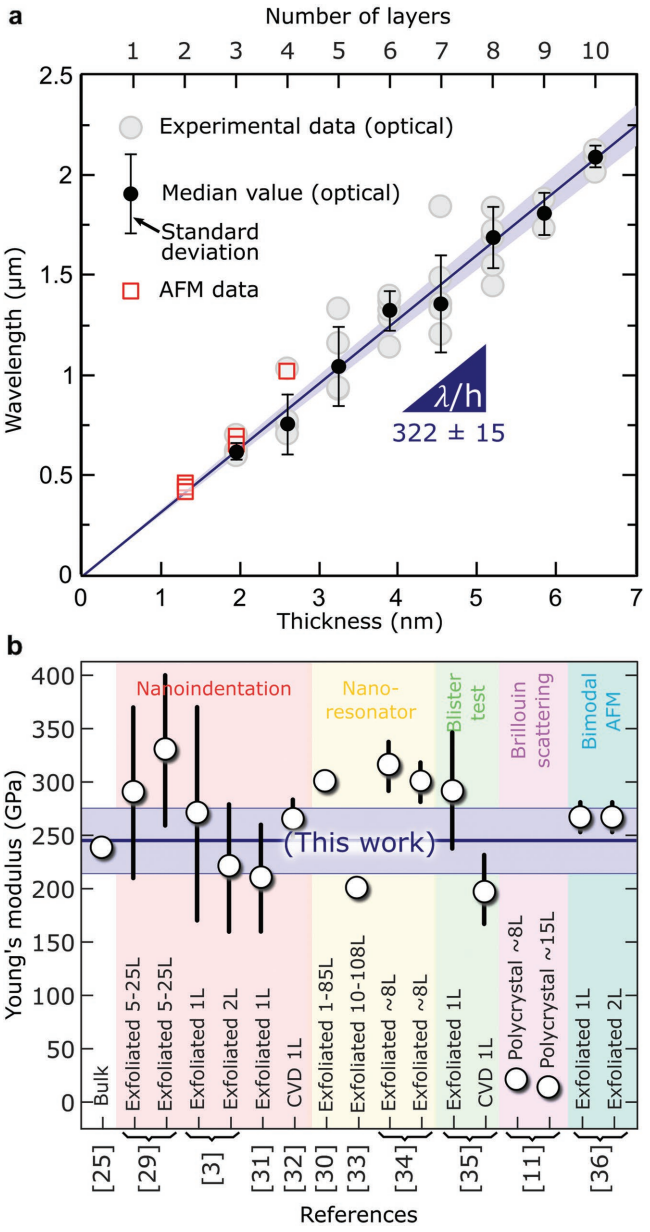

Figure 3. a) Relationship between the wavelength of the ripples and the thickness of the MoS_2 flakes. The solid dark blue line represents a linear fit to the experimental data; the shaded light blue area around it indicates the uncertainty of the fit. The slope of the wavelength versus thickness relationship, from which the Young's modulus of MoS_2 can be determined, is also included in the plot. b) Summary of the values for the MoS_2 Young's modulus, reported in in the literature and their comparison with the value obtained in this work (solid dark blue line, the shaded light blue area indicates the uncertainty) $E = 246 \pm 35$ GPa. Details about the sample fabrication and the measurement technique for the reference data points have been included in the plot.

available in the literature. In the figure we specified the testing method and the sample fabrication method. The value determined with the buckling metrology method is in good agreement with the bulk value of MoS_2, measured by neutron dispersion and X-ray diffraction measurements, and it is compatible within experimental uncertainties with most of recent works that studied

ultrathin flakes through nanoindentation, the analysis of the dynamics of nanomechanical resonators, the microscopic version of the blister test and bimodal atomic force microscopy.[3,11,25,29–36] The only noticeable disagreement is with the values reported in ref.[11], measured with a microscopic version of Brillouin light scattering. In that reference, however, the authors measured a polycrystalline sample fabricated by direct sulfurization of a metallic film whose mechanical properties are expected to be dominated by the presence of defects. All the information contained in Figure 3b is also summarized in **Table 1** to facilitate a quantitative comparison between the different methods.

Table 1 also summarizes values reported in the literature for other TMDCs ($MoSe_2$, WS_2, and WSe_2)[32,10,37] and directly compares these literature values with the ones obtained by repeating the process described above for MoS_2 for the other members of the transition metal dichalcogenide family (see Supporting Information). From the comparison between the S- and Se-based TMDCs there is a clear trend: the Young's modulus of the S-based TMDCs is larger than that of Se-based ones. This trend is in good agreement with ab initio calculations.[26,38]

It is important to make a critical comparison between the different experimental techniques employed to determine the Young's modulus values of 2D materials. In **Table 2** we present key information about the requirements needed by these different methods for the sample fabrication and the measurement process as well as a coarse estimation of the time needed for those processes. The first noticeable difference is that unlike the other methods, the buckling metrology method does not require any lithographic process. On the other hand, the nanoindentation, the nanomechanical resonator-based method, the micro-blister test, the microscopic version of the tensile test, and the micro-Brillouin light scattering require to fabricate freely suspended nanosheets, which significantly increases the complexity of the fabrication process and the time involved and it decreases the success yield. Moreover, we stress that the requirement of expensive lithography and etching setups necessary to fabricate the suspended sheets might be highly restrictive by preventing the implementation of these methods in many research groups without access to cleanroom facilities. The nanomechanical resonator-based method also requires the use of a specialized experimental setup for the measurement of the mechanical properties of the flakes, which again can be a handicap for its implementation in many research groups. The micro-Brillouin scattering method also

Table 1. Summary of values for the Young's modulus (and their uncertainties) reported in the literature for MoS_2, $MoSe_2$, WS_2, and WSe_2. The testing methods as well as some characteristics of the studied samples (fabrication method and number of layers) are highlighted in the table to facilitate the comparison between the different reported values.

Material	Testing method	Sample		E [GPa]	Reference
		Isolation method	# of layers		
MoS_2	Brillouin scattering	Bulk natural crystal		238	[25]
	Nanoindentation	Exfoliation (natural)	5 to 25	290 ± 80	[29]
			5 to 25	330 ± 70	[29]
			1	270 ± 100	[3]
			2	220 ± 60	[3]
			1	210 ± 50	[31]
		CVD	1 to 2	264 ± 18	[32]
	Dynamics of mechanical resonator	Exfoliation (natural)	1 to 85	300	[30]
			10 to 108	200	[33]
			≈8	315 ± 23	[34]
			≈8	300 ± 18	[34]
	Micro-Buggle test	Exfoliation (natural)	1	292 ± 54	[35]
		CVD	1	197 ± 31	[35]
	Micro-Brillouin light scattering	CVD-poly	≈8	20.1 ± 3.2	[11]
			≈15	13.7 ± 2	[11]
	Bimodal AFM	Exfoliation (natural)	1	265 ± 13	[36]
			2	265 ± 13	[36]
	Buckling metrology method	**Exfoliation (natural)**	**3 to 11**	**246 ± 35**	**This work**
$MoSe_2$	Micro-tensile test	CVD	1 to 2	177.2 ± 9.3	[10]
	Buckling metrology method	**Exfoliation (synthetic)**	**5 to 10**	**224 ± 41**	**This work**
WS_2	Nanoindentation	CVD	1	272 ± 18	[32]
	Buckling metrology method	**Exfoliation (synthetic)**	**3 to 8**	**236 ± 65**	**This work**
WSe_2	Nanoindentation	Exfoliation (synthetic)	5 to 12	167 ± 7	[37]
	Buckling metrology method	**Exfoliation (synthetic)**	**4 to 9**	**163 ± 39**	**This work**

Table 2. Critical comparison between the different methods reported in the literature to test the mechanical properties of 2D materials. Key requirements for the sample fabrication and the measurement process are indicated as well as a qualitative estimation of the time needed in these processes and the complexity of the implementation (indicated with the symbol "●", the more symbols the more time/complexity is needed).

Technique	Sample fabrication		Measurement		Complexity	Cost	Ref.
	Requirements	Time	Requirements	Time			
Nanoindentation	Lithography + flake transfer	●●	AFM Air atmosphere	●●	●●	●●	[2,3,29,31,32]
Nanomechanical resonator	Lithography + flake transfer	●●	Interferometer (or electrical read-out) High frequency electronics High vacuum	●●	●●●	●●	[30,33,34]
Micro-blister test	Lithography + flake transfer + high pressure chamber	●●●	AFM Air atmosphere	●●●	●●●	●●	[35]
Micro-Brillouin scattering	Lithography + flake transfer	●●	Modified micro-Raman spectrometer Air atmosphere	●●	●●	●●	[11]
Micro-tensile test	Lithography + flake transfer	●●●	SEM High vacuum	●●	●●●	●●●	[10]
Bimodal AFM	Direct exfoliation on substrate	●	AFM Air atmosphere	●	●●	●●	[36]
Buckling metrology method	**Direct exfoliation on substrate**	●	**Optical microscope** **Air atmosphere** **Multiple flakes**[a)]	●●*	●	●	**This work**

[a)]Multiple flakes are needed in the buckling metrology method to reduce the experimental uncertainty (see the main text).

needs a very specialized equipment.[11] The sample fabrication of the buckling metrology method, on the other hand, does not require any specialized technique as it simply relies on the exfoliation of the 2D materials on top of the stressed elastomer substrate and an optical microscope. Common to all the methods is the need to determine the number of layers, which can be done with atomic force microscopy (time needed for the measurement ≈30–60 min) or optical microscopy (≈1–10 min).

In summary, the buckling metrology method provides a fast and easy way of measuring the mechanical properties of 2D materials as compared with conventionally employed approaches (nanoindentation, nanomechanical resonators, blister test, and micro-Brillouin light scattering). We demonstrate this method with MoS_2, $MoSe_2$, WS_2 and WSe_2 and found that it provides Young's modulus values in good agreement with the literature values. Because of its simplicity, the fast measurement speed, and straightforwardness of the data analysis we believe that this method can be a highly attractive way to study the mechanical properties of 2D materials.

NOTE: During the elaboration of this manuscript we became aware of a recent publication where another technique to measure the mechanical properties of supported (not freely suspended) 2D materials was developed.[36] The mechanical properties of single- and bilayer MoS_2 supported onto a SiO_2/Si surface were measured with a bimodal AFM. The technique relies in the use of a multifrequency AFM in combination with finite elements analysis in order to extract Young's modulus.

Experimental Section

Materials: MoS_2 samples were prepared out of a bulk natural molybdenite crystal (Moly Hill mine, Quebec, Canada). $MoSe_2$ and WSe_2 samples were prepared out of bulk synthetic crystals grown by physical vapor transport method (provided by Prof. Rudolf Bratschitsch). WS_2 samples were prepared out of a bulk synthetic crystal grown by physical vapor transport method at Tennessee Crystal Center. The elastomer substrate used in this work is a commercially available polydimethylsiloxane-based substrate manufactured by Gel-Pak (both Gel-Film WF X4 6.0 mil and Gel-Film PF X4 6.5 mil were used with identical results).

Determination of the Young's modulus of the Gel-Film substrate: The Young's modulus of the elastomeric substrate was determined by means of a force versus elongation experiment where different forces are applied to a Gel-Film strip ($63.5 \times 10 \times 0.165$ mm) by loading different test masses at one end of the strip and monitoring the relative changes in length upon loading though a Canon EOS 1200D camera equipped with a EF-S 18-55 DC III objective lens. See Supporting Information for more details.

Optical microscopy: Optical microscopy images were acquired with an AM Scope BA MET310-T upright metallurgical microscope equipped with an AM Scope mu1803 camera with 18 megapixels. The calibration of the optical magnification system was carried out by imaging standard samples: one CD, one DVD, one DVD-R, and two diffraction gratings with 300 lines/mm (Thorlabs GR13-0305) and 600 lines/mm (Thorlabs GR13-0605). See details about the calibration in Supporting Information.

Image analysis: The quantitative analysis of the transmittance of the flakes and the rippling wavelength has been carried out using Gwyddion software.[38]

Thickness determination: The thickness determination was carried out by extracting the transmittance of the blue channel of the transmission mode optical microscopy images and comparing it with the results of a reference (not-buckled) sample. See Supporting Information for more details.

Atomic Force Microscopy (AFM): Atomic force microscopy measurements were carried out with an ezAFM from NanoMagnetics Instruments operated in tapping mode with cantilevers of 40 N m^{-1} and a resonance frequency of 300 kHz.

Supporting Information

Supporting Information is available from the Wiley Online Library or from the author.

Acknowledgements

This project received funding from the European Research Council (ERC) under the European Union's Horizon 2020 research and innovation programme (grant agreement n°755655, ERC-StG 2017 project 2D-TOPSENSE) and the European Union's Horizon 2020 Graphene Flagship funding (Grant Graphene Core2 785219).

Conflict of Interest

The authors declare no conflict of interest.

Keywords

2D materials, mechanical properties, nanomechanics, transition metal dichalcogenides, Young's modulus

Received: November 5, 2018
Revised: December 14, 2018
Published online: January 7, 2019

[1] D. Akinwande, N. Petrone, J. Hone, *Nat. Commun.* **2014**, *5*, 5678.
[2] C. Lee, X. Wei, J. W. Kysar, J. Hone, *Science* **2008**, *321*, 385.
[3] S. Bertolazzi, J. Brivio, A. Kis, *ACS Nano* **2011**, *5*, 9703.
[4] B. Radisavljevic, A. Radenovic, J. Brivio, V. Giacometti, A. Kis, *Nat. Nanotechnol.* **2011**, *6*, 147.
[5] Q. H. Wang, K. Kalantar-Zadeh, A. Kis, J. N. Coleman, M. S. Strano, *Nat. Nanotechnol.* **2012**, *7*, 699.
[6] M. Poot, H. S. J. van der Zant, *Appl. Phys. Lett.* **2008**, *92*, 063111.
[7] C. Gómez-Navarro, M. Burghard, K. Kern, *Nano Lett.* **2008**, *8*, 2045.
[8] I. W. Frank, D. M. Tanenbaum, A. M. van der Zande, P. L. McEuen, *J. Vac. Sci. Technol., B: Microelectron. Nanometer Struct.* **2007**, *25*, 2558.
[9] J. S. Bunch, A. M. van der Zande, S. S. Verbridge, I. W. Frank, D. M. Tanenbaum, J. M. Parpia, H. G. Craighead, P. L. McEuen, *Science* **2007**, *315*, 490.
[10] Y. Yang, X. Li, M. Wen, E. Hacopian, W. Chen, Y. Gong, J. Zhang, B. Li, W. Zhou, P. M. Ajayan, Q. Chen, T. Zhu, J. Lou, *Adv. Mater.* **2017**, *29*, 1604201.
[11] B. Graczykowski, M. Sledzinska, M. Placidi, D. Saleta Reig, M. Kasprzak, F. Alzina, C. M. Sotomayor Torres, *Nano Lett.* **2017**, *17*, 7647.
[12] A. Castellanos-Gomez, V. Singh, H. S. J. van der Zant, G. A. Steele, *Ann. Phys.* **2015**, *527*, 27.
[13] X. Li, M. Sun, C. Shan, Q. Chen, X. Wei, *Adv. Mater. Interfaces* **2018**, *5*, 1701246.
[14] C. M. Stafford, C. Harrison, K. L. Beers, A. Karim, E. J. Amis, M. R. VanLandingham, H.-C. Kim, W. Volksen, R. D. Miller, E. E. Simonyi, *Nat. Mater.* **2004**, *3*, 545.
[15] N. Bowden, S. Brittain, A. G. Evans, J. W. Hutchinson, G. M. Whitesides, *Nature* **1998**, *393*, 146.
[16] M. A. Reyes-Martinez, A. Ramasubramaniam, A. L. Briseno, A. J. Crosby, *Adv. Mater.* **2012**, *24*, 5548.
[17] P. Feicht, R. Siegel, H. Thurn, J. W. Neubauer, M. Seuss, T. Szabó, A. V Talyzin, C. E. Halbig, S. Eigler, D. A. Kunz, *Carbon* **2017**, *114*, 700.
[18] D. A. Kunz, J. Erath, D. Kluge, H. Thurn, B. Putz, A. Fery, J. Breu, *ACS Appl. Mater. Interfaces* **2013**, *5*, 5851.
[19] D. A. Kunz, P. Feicht, S. Gödrich, H. Thurn, G. Papastavrou, A. Fery, J. Breu, *Adv. Mater.* **2013**, *25*, 1337.
[20] C. J. Brennan, J. Nguyen, E. T. Yu, N. Lu, *Adv. Mater. Interfaces* **2015**, *2*, 1500176.
[21] A. L. Volynskii, S. Bazhenov, O. V Lebedeva, N. F. Bakeev, *J. Mater. Sci.* **2000**, *35*, 547.
[22] D. Khang, J. A. Rogers, H. H. Lee, *Adv. Funct. Mater.* **2009**, *19*, 1526.
[23] Y. Niu, S. Gonzalez-Abad, R. Frisenda, P. Marauhn, M. Drüppel, P. Gant, R. Schmidt, N. Taghavi, D. Barcons, A. Molina-Mendoza, S. de Vasconcellos, R. Bratschitsch, D. Perez De Lara, M. Rohlfing, A. Castellanos-Gomez, *Nanomaterials* **2018**, *8*, 725.
[24] R. H. Pritchard, P. Lava, D. Debruyne, E. M. Terentjev, *Soft Matter* **2013**, *9*, 6037.
[25] J. L. Feldman, *J. Phys. Chem. Solids* **1976**, *37*, 1141.
[26] D. Çakır, F. M. Peeters, C. Sevik, *Appl. Phys. Lett.* **2014**, *104*, 203110.
[27] I. D. Johnston, D. K. McCluskey, C. K. L. Tan, M. C. Tracey, *J. Micromech. Microeng.* **2014**, *24*, 035017.
[28] K. Khanafer, A. Duprey, M. Schlicht, R. Berguer, *Biomed. Microdevices* **2009**, *11*, 503.
[29] A. Castellanos-Gomez, M. Poot, G. A. Steele, H. S. J. van der Zant, N. Agraït, G. Rubio-Bollinger, *Adv. Mater.* **2012**, *24*, 772.
[30] A. Castellanos-Gomez, R. van Leeuwen, M. Buscema, H. S. J. van der Zant, G. A. Steele, W. J. Venstra, *Adv. Mater.* **2013**, *25*, 6719.
[31] R. C. Cooper, C. Lee, C. A. Marianetti, X. Wei, J. Hone, J. W. Kysar, *Phys. Rev. B* **2013**, *87*, 035423.
[32] K. Liu, Q. Yan, M. Chen, W. Fan, Y. Sun, J. Suh, D. Fu, S. Lee, J. Zhou, S. Tongay, *Nano Lett.* **2014**, *14*, 5097.
[33] J. Lee, Z. Wang, K. He, J. Shan, P. X.-L. Feng, *ACS Nano* **2013**, *7*, 6086.
[34] D. Davidovikj, F. Alijani, S. J. Cartamil-Bueno, H. S. J. Zant, M. Amabili, P. G. Steeneken, *Nat. Commun.* **2017**, *8*, 1253.
[35] D. Lloyd, X. Liu, N. Boddeti, L. Cantley, R. Long, M. L. Dunn, J. S. Bunch, *Nano Lett.* **2017**, *17*, 5329.
[36] Y. Li, C. Yu, Y. Gan, P. Jiang, J. Yu, Y. Ou, D.-F. Zou, C. Huang, J. Wang, T. Jia, *npj Comput. Mater.* **2018**, *4*, 49.
[37] R. Zhang, V. Koutsos, R. Cheung, *Appl. Phys. Lett.* **2016**, *108*, 042104.
[38] Z. Fan, Z. Wei-Bing, T. Bi-Yu, *Chin. Phys. B* **2015**, *24*, 097103.

